Extending the environmental benefits of ethanol–diesel blends through DGE incorporation

Herreros, J. M. , Schroer, K. , Sukjit, E. and Tsolakis, A.

Original citation & hyperlink:
Herreros, J. M. , Schroer, K. , Sukjit, E. and Tsolakis, A. (2015) Extending the environmental benefits of ethanol–diesel blends through DGE incorporation. Applied Energy, volume 146 : 335–343
http://dx.doi.org/10.1016/j.apenergy.2015.02.075

DOI 10.1016/j.apenergy.2015.02.075
ISSN 0306-2619

Publisher: Elsevier

Extending the environmental benefits of ethanol-diesel blends through DGE incorporation

J.M. Herreros, K. Schroer, E. Sukjit and A. Tsolakis*

School of Mechanical Engineering, University of Birmingham, B15 2TT, UK

*Corresponding Author: Tel.: +44 (0) 121 414 4170, Fax : +44 (0) 121 414 7484

Email Address: a.tsolakis@bham.ac.uk

Abstract

This research focuses on the potential use of DGE (diethylene glycol diethyl ether), as a high-cetane number oxygenated additive to diesel-like fuels. Apart from evaluating its individual effects an investigation of how DGE can facilitate the use of bio-ethanol in diesel engines was conducted; which faces many technical difficulties, but can provide environmental advantages over biodiesel and conventional diesel fuel. Four partly renewable fuel blends with varying contents of DGE and ethanol were designed with overall diesel-replacement rate of 20%.

DGE was found to reduce gaseous emissions, achieving a simultaneous reduction in both soot and NO_x which highlighted the beneficial effects of its high cetane number and oxygen content. In ethanol-diesel blends small additions of DGE significantly enhanced blend stability and blend auto-ignition properties. Improvements in the NO_x/soot trade-off characteristics were obtained for all blends. All tested blends produced lower particulate matter number concentrations and soot with characteristics that reduced their oxidation temperatures, hence providing benefits for diesel particulate filter regeneration. Overall it was found that DGE provides considerable energy and environmental benefits if used both as a single oxygenate with diesel or in multicomponent blends with ethanol and diesel.

Keywords: diesel combustion, ether, ethanol blends, NO_x-soot trade-off, soot oxidation

Acronyms and Abbreviations

CAD	Crank angle degree	LHV	Lower heating value
CO	Carbon monoxide	NO_x	Oxides of nitrogen (NO, NO_2)
CO_2	Carbon dioxide	PM	Particulate matter
DGE	Diethylene glycol diethyl ether	RME	Rapeseed methyl ester
DGM	Diethylene glycol dimethyl ether	ROHR	Rate of heat release
DPF	Diesel particulate filter	SOF	Soluble organic fraction
E	Ethanol	SOM	Soluble organic material
EGR	Exhaust gas recirculation	TDC	Top dead centre
FTIR	Fourier-transform infrared spectroscopy	THC	Total hydrocarbon
HC	Hydrocarbon	TGA	Thermogravimetric Analyser
HFRR	High frequency reciprocating rig	ULSD	Ultralow sulphur diesel
IETE	Indicated engine thermal efficiency	B5	Ultralow sulphur diesel +5% RME
IMEP	Indicated mean effective pressure	VOM	Volatile organic material
ISFC	Indicated specific fuel consumption		

1. Introduction

There is an increased interest in searching for alternatives energy carriers in the transportation and energy generation sectors over the past decade. The motivations for that are the reduction of the fossil fuels dependence (energy sustainability), a desire to reduce greenhouse gas emissions (especially CO_2 in the transportation sector) and human health concerns related to other pollutant emissions (particulate matter, NO_X, CO, etc.). In fact, in a recent press release, the International Agency for Research on Cancer (IARC) classified diesel exhaust as carcinogenic to humans (Group 1). Due to these issues new legislation is being introduced to promote the use of biofuels in the transportation sector and strict pollutant emission regulations must be fulfilled demanding the incorporation of aftertreatment systems.. These short and medium term scenarios indicate the ideal timeliness for research aiming to design new energy alternatives able to overcome those energy and environmental issues taking into account the interaction between some of the vehicle systems (e.g. the effect of alternative fuels in the diesel particulate filter).

Efforts to tackle these challenges have been based on both engine and fuel-focused techniques. Diesel reformulation using sustainably sourced biofuels seems to be a promising field of research. The focus now lies on biofuels obtained from non-edible feedstock leading to several publications critically assessing the production and environmental implications of energy alternatives derived from algae [1]-[2], triglycerides [3], lignocellulose [4]-[5], etc. A feasible and common alternative could be the use of primary alcohols such us methanol [6], ethanol [7], butanol [8] and/or pentanol [9]. Traditionally, ethanol is the one which more attention has received as it could be produced from non-edible feedstock and it has some advantages over biodiesel in terms of availability, price and emission characteristics. Its oxygen content is about three times higher than biodiesel resulting in further improvements in PM emissions [10]-[11] and it has been demonstrated to reduce NO_x emissions under certain operating conditions [12]. However various limitations in the use of ethanol in compression ignition (CI) engines exist due to its adverse effects on some key fuel properties in particular flash-point [13], blend stability with diesel-like fuels, viscosity, lubricity and cetane number [12]-[15]. For high ethanol content in diesel blends (i.e. e-diesel) cetane-enhancing and stability-improving components must be utilised [16] such as biodiesel **Error! Reference source not found.**-[18].

Diethylene glycol diethyl ether (DGE) could be a promising fuel additive for compression ignition engines based on its high cetane number and its high amounts of fuel-born oxygen. These properties also qualify DGE as a potential cetane-enhancing additive to e-diesel blends. A review of the limited literature suggests that DGE may have similar effects to DGM, a well-studied [17]-[18] but about three-times more expensive oxygenate. When combusting pure DGE under EGR conditions in a diesel engine, Cheng et al. obtained reductions in all regulated emissions as compared to neat diesel [23] which was confirmed in two other studies by Upatnieks et al. who attributed this to the high oxygen content and low soot formation potential of DGE [24][25]. Yet the available literature on DGE fails to give a detailed account of the additive's real-world potential in diesel combustion as there are no in-depth studies on its combustion pattern and detailed emission characteristics. The factual novelty of this work, however, is the

enhancement of ethanol-diesel blends through the incorporation of DGE which has so far not been attempted.

The aim of this investigation is to evaluate the potential of DGE as a diesel additive with a view towards designing new feasible fuel blends composed of different hydrocarbon constituents to partly replace diesel fuel while obtaining energy efficiency improvements and environmental benefits. In doing so the effects of various fuel blends on engine performance, combustion patterns, exhaust emissions and aftertreatment systems are investigated.

2. Material and Methods

2.1 Test Engine and Instrumentation

For this research a natural aspirated single-cylinder diesel engine was utilised. The research engine employs a pump-line nozzle direct injection system with mechanical injection timing. The injector has 3 holes with 0.25mm diameter each, while the opening injection pressure is 180 bar. Injection timing was not optimised for the different fuel blends. A Thrige Titan DC electric dynamometer with a load cell and a thyristor controlled Shackleton System Drive was used to load and motor the engine.

Each fuel was tested at constant engine speed (1500 rpm) and two different load conditions of 3 bar and 5 bar indicated mean effective pressure (IMEP) representing ~30% and ~70% of the engine's power capacity respectively. Additionally exhaust gas recirculation (EGR) of 0%, 10% and 20% was introduced for both loads to study its effect on emissions. The results and error bars showed in the graphs are calculated from three measurements for every studied fuel blend and engine operating condition. A calibrated glass bulb, connected in parallel with the fuel tank, was used to determine the liquid fuel flow by timing the consumption of a known volume of fuel. The volumetric fuel consumption was converted into mass fuel consumption using the density values of the fuels.

In-cylinder pressure traces were acquired by a Kistler 6125B quartz type pressure transducer mounted at the cylinder head and a Kistler 5011 charge amplifier at crank shaft positions determined by a 360-ppr

incremental shaft encoder with data recorded by a National Instruments PCI-MIO-16E-4 data acquisition board installed in a PC. In-house developed LabVIEW based software was used to obtain pressure data and combustion parameters were calculated based on 200 consecutive engine cycles after they were conditioned and smoothed (e.g. coefficient of variation – COV of IMEP, peak pressure, indicated power and heat release). The COV of IMEP was always below 5% and the COV of peak pressure was always below 2%.

The apparent heat release rate was calculated using the following equation:

$$\frac{dQ}{d\theta} = \frac{\gamma}{\gamma - 1} p \frac{dV}{d\theta} + \frac{1}{\gamma - 1} V \frac{dp}{d\theta}$$

Where, γ is the ratio of specific heats (Cp/CV), p is the instantaneous in-cylinder pressure and V is the instantaneous engine cylinder volume. The values of γ are calculated by interpolation based on the actual p-V diagrams. It is worthy to notice that in the literature there are advanced models which consider the instantaneous in-cylinder composition to calculate rate of heat release and in-cylinder mean combustion temperature [26]. Those advanced models has not been considered here, while they will be taken into consideration for further work in order to more accurately calculate gross and net rate of heat release as well as mean in-cylinder temperature."

The engine exhaust emission analysis was focused on soot, PM, NO_x, THC, CO and CO_2. An in-depth investigation of particulate matter (PM) was carried out. Fourier Transform Infrared (FTIR) gas analyser from MKS was used to measure gaseous emissions. An additional Horiba Mexa 7100DEGR analyser was employed to measure the concentrations of NOx, CO, CO_2, O_2 and THCs. The analyser measures NOx ($NO + NO_2$) by chemiluminescence, CO and CO_2 are measured using non-dispersive infrared (NDIR), O_2 by an electrochemical method and hydrocarbons (THCs) by flame ionisation detection (FID). A Horiba Mexa-1230 PM analyser was employed to determine soot, SOM (soluble organic material), SOF (soluble organic fraction), and the total amount of PM in the exhaust. Secondly a TSI scanning mobility particle sizer (SMPS) 3080 electrostatic classifier was used to establish the particle size distribution. The sample was thermo-diluted using a rotating disk, with the dilution ratio set to 200:1 at 150°C. Finally PM was

collected on glass filters using an in-house ejector diluter (8:1 dilution ratio) drawing diluted exhaust gas through the filter at 10 l/min for 60 min. The filters were analysed in a Perkin-Elmer Pyris 1 TGA thermogravimetric analyser following the method described by Gill et al. [22].

2.2 Fuel blends selection

As discussed above there are some crucial fuel properties which are adversely affected by the addition of ethanol (e.g. blend stability, cetane number, lubricity, etc.). Prior to choosing blend compositions for engine tests these limiting factors were further investigated and compared with the applicable European standard for diesel fuels EN 590:2009 [27].

The miscibility of DGE with ULSD and ethanol was studied by preparing multiple diesel blends with different DGE contents and storing them at temperatures from +10 °C to -5 °C. Previous research into the stability of diesel-ethanol blends concluded that blends of ULSD and 20% ethanol become unstable at temperatures below 20 °C [8]. In this work the beneficial effects of the DGE on ethanol-diesel blend stability was investigated. The incorporation of 5% DGE enables to obtain stable 20% ethanol - diesel blends at temperatures as low as -5°C. The minimum and maximum viscosity limits are 2.00 and 4.50 cSt respectively. Referring to Table 1 it is apparent that this limit is not infringed by the replacement of just 20% of the base fuel with DGE or ethanol. Lubricity was measured using a PCS Systems High Frequency Reciprocating Rig (HFRR). The corrected wear scar diameter obtained in this test must not exceed 460 μm [28]. Earlier investigations indicated that blends with DGE content above 15% exceeded this permitted limit. The incorporation of ethanol in these blends is expected to reduce blend lubricity further due to the poor lubricity properties of ethanol [14]. This would result in overall diesel replacement rates of just around 10%. To overcome this limitation 5% of Rapeseed methyl ester biodiesel (RME) was added to the diesel fuel (subsequently called B5) in order to improve the lubricity of alcohol-diesel blends [29]-[30]. Further tests confirmed that this small addition of RME eliminates the problem of lubricity for diesel replacement rates with ethanol of up to 30% (see Figure 1).

In line with the research aim and objectives four blends were prepared. To study the effects of DGE on combustion and emissions a DGE-B5 blend was prepared. To investigate how DGE can improve e-diesel blends three tertiary blends with varying contents of DGE and ethanol were created. For all four blends the overall diesel replacement rate was 20%. While the ethanol content was increased step by step in increments of 5%, the DGE content was decreased stepwise by the same percentage. As a result, the total oxygen content was at similar levels for the blends, diminishing the total oxygen content effect when blends are compared. The four test blends were compared with the B5 reference fuel. ULSD, RME and Ethanol were obtained from Shell Global Solutions (UK) while DGE was sourced from Sigma-Aldrich. Relevant fuel properties have been measured and/or found in the relevant literature [29], [31]-[33] as it is detailed in Table 1. It was again verified that the aforementioned key blend properties complied with the standard.

3. Results and Discussion

3.1 Performance Parameters

Figure 2 (a) shows the indicated thermal efficiency (ITE), the ratio of the engine's indicated power output to the flow fuel's energy content (mass fuel consumption times fuel's lower heating value). On one hand, the fuel consumption is increased for all blends as compared to the B5 reference fuel. On the other hand, the heating value of the blends is lower than the heating value of B5. The increased in specific fuel consumption for the blends are lower than the decrease in heating value [34] slightly increasing indicated thermal efficiency. Studies have shown that this increase is mainly due to the oxygenated nature of the fuel additives [35]. The increased oxygen availability achieves a more complete combustion even in fuel-rich regions. Additionally it can be seen that all blends achieve nearly identical efficiencies which seems to confirm the correlation between oxygen mass fraction and thermal efficiency as described in prior studies.

3.2 Combustion Characteristics

In Figure 2 (b) the in-cylinder pressure and rate of heat release (ROHR) for the operating load of 3 bar IMEP are plotted against the crank angle degree for 0% EGR. The shortest ignition delay was observed for 20DGE followed by 15DGE5E, B5, 10DGE10E and finally 5DGE15E. The start of combustion of the 5DGE15Ethanol blend is 6CAD bTDC, when ethanol is substituted by DGE for the 10DGE10Ethanol and 15DGE5Ethanol the start of combustion is advanced to 7 and 8CAD bTDC, respectively. This behaviour qualitatively follows the differences in estimated cetane numbers [36],[37] when fuel molar fractions are considered. However, when cetane number estimation is based on mass fraction, all the fuel blend's cetane values are higher than those of B5 which does not correspond to the delay time experimentally observed. The above discussed results, lead to conclude that the estimation based on molar fraction better reflects the autoignition properties of a multi-fuel blend when the components have very different molecular masses (e.g. ethanol, diesel and DGE).

The combustion process is generally characterised by an initial pre-mixed combustion (the first heat released peak [38]) followed by a diffusion combustion phase [39]. The intensity of these phases varies considerably across the different blends. The 5DGE15E-blend has the largest pre-mixed combustion phase resulting in the largest heat release peak. The long ignition delay allows the fuel to mix well with the air leading to a more homogenous initial combustion [38]. 20DGE has the smallest premixed combustion phase for both load conditions due to its short ignition delay. Also, as has been concluded in various studies under similar mode of combustion the higher the degree of premixed combustion, the higher the peak pressure [23],[38]. This is the case for the 3 bar condition and applies also to the 5 bar condition.

3.3 Gaseous Carbonaceous Emissions

The THC emissions of all blends at both engine operating loads (Figures 3 and 4) are lower than those of B5. This can be attributed to the higher oxygen content of the fuels which causes a cleaner and more complete combustion [6],[34],[40]. 20DGE and 15DGE5E show the lowest overall THC emissions while the THC emissions of 5DGE15E are the highest of the studied blends. The increase of hydrocarbon emissions when ethanol is used it has been previously reported in the literature [14],[17],[18],[31]. The

main reasons for the higher unburnt hydrocarbon emissions when the ethanol content is higher could be i) the higher cetane number of these blends that lead to an advanced combustion resulting in more available time to completely oxidise hydrocarbons and CO [34],[41] ii) the high enthalpy of vaporisation of ethanol which will result in a reduction in the in-cylinder combustion temperature inhibiting the hydrocarbon oxidation [31]. The specific THC emissions are generally lower at high loads. This is most likely due to increased peak pressures resulting in a more complete combustion.

CO emissions demonstrate a very similar qualitative behaviour to THC emissions. Again the results can be explained by referring to oxygen content, enthalpy of vaporisation and cetane number. The emissions for three of the four blends are clearly reduced as compared to B5 at both 3 bar and 5 bar IMEP due to their higher oxygen content [22],[23],[38]. The 5DGE15E blend produced higher CO emissions than B5. This is thought to be a result of its lower cetane number and consequently retarded combustion phasing. Various studies into the field have found that lower cetane numbers tend to increase CO emissions, an effect which has been attributed to the resulting retarded combustion allowing less time for the fuel and intermediate species to combust completely [42],[43]. For this blend the negative effects of a lower CN number seem to outweigh the positive effects of increased oxygenation in terms of CO emissions.

3.4 Nitrogen Oxides (NO_x) Emissions

NO_x emissions for the studied blends compared to B5 are shown in Figure 3 and 4. To explain the different trends across the studied blends four main factors are considered: fuel-born oxygen, ignition delay, the ratio of premixed to diffusion combustion and the enthalpy of evaporation.

It has been previously reported that the presence of fuel-born oxygen could increase NO_x emissions. The oxygen in the fuel could promote the NO formation reaction [34],[44] and reduce the heat losses by soot radiation resulting in higher in-cylinder combustion temperature [34],[42]. Furthermore, the larger premixed combustion phase resulting in higher peak pressures and temperatures also promote NO_x formation. These two factors could explain why the combustion of two of the four blends (15DGE5E and 10DGE10E) show significantly higher emissions of NO_x than the combustion of B5 and rest of the tested

fuel blends. However, the 5DGE15E blend exhibits a decrease in NO_x emissions compared to 10DGE10E although its premixed phase is larger. A possible explanation is the higher ethanol content in the blend. Ethanol has a high enthalpy of evaporation causing temperatures to decrease during combustion [31]. This effect seems to counteract the influence of the premixed combustion and higher oxygen content for this blend while it seems not to be strong enough in the blends containing only 5% and 10% of ethanol. In the case of 20DGE, the lower premixed-to-diffusion-combustion ratio is the dominant factor leading to lower peak pressures (as can be observed in Figure 2 (b)) and thus lower NO_x levels.

3.5 Particulate Matter (PM) emissions and their composition

Particulate Matter is composed of two main fractions: i) soot which is solid carbonaceous material and ii) soluble organic material which are adsorbed/condensed hydrocarbons onto the soot particles' surface [45] (PM = Soot + SOM). The SOF is defined as the proportion of SOM in total PM (SOF = SOM/PM).

In addition to the gaseous emissions, soot results can be found in Figures 3 and 4. It can be seen that all four blends show reductions in soot emissions for both engine loads. The most important reason for this is the increased oxygenation of the fuels [12],[22],[31],[34]-[35]. Increased oxygen availability means better and more complete fuel combustion even in fuel-rich regions and promotes the oxidation of already formed soot [34]. However oxygen content cannot be the only determinant of soot as the absolute soot reductions vary across the blends although their oxygen mass fractions are nearly the same. To explain why 20DGE has one of the smallest soot emissions the effect of DGE as an ether must be considered. Westbrook et al. [46] have suggested that ethers strongly inhibit soot emissions due to their atomic structure in which one oxygen atom is bonded to two carbon atoms. This way less carbon atoms are available for soot production. Another crucial factor in soot emissions is the ignition delay of a fuel. A retarded combustion tends to increase soot as there is less time for soot oxidation which is especially the case for the 10DGE10E blend. However, for the 5DGE15E blend the negative effects of an even further retarded combustion as well as much lower ether content seem to be outweighed by the positive effect of a much longer premixed combustion phase. Better premixing tends to eliminate fuel rich regions where soot

is primarily produced. As a result soot emissions for 5DGE15E are lower than in the case of B5, 15DGE5E and 10DGE10E at both operating pressures.

In terms of PM composition, in Figure 5 it can be observed that 20DGE has the highest SOF closely followed by 5DGE15E. The increase in SOF is mainly driven by the low level of soot associated with the combustion of those blends (see Figure 3 and 4) rather by a higher emission of volatile organic material (VOM). However, 15DGE5E and 10DGE10E display similar SOF with respect to B5 although their soot emissions are lower which can be explained by a simultaneous reduction in SOM and soot and thus an overall reduction in total PM as compared to B5. When comparing engine load and EGR, SOF decreases with an increase in engine load and EGR. This is again due to an increase in soot emissions derived from the combustion at high engine load and EGR levels.

3.6 NO_x /Soot Trade-off under EGR conditions

NO_x and soot emissions for different EGR operating conditions are depicted in Figure 6. As can be seen EGR reduces NO_x but increases soot (trade-off) mainly due to the decreased oxygen availability in the combustion chamber. It is apparent that all blends display improved trade-off characteristics as compared to B5 as they lie below the B5 trade-off curve, with 20DGE and 5DGE15E appears to have the best trade-off relationship. Trade-off improvements with fuel blends (as indicated by the slope of the lines) seem to be best for low EGR additions (eg. 10%). Higher EGR percentage further reduces NO_x emissions, however the incurred soot penalty is much higher (higher slope of the line from 10 to 20% EGR in comparison to the slope from 0 to 10% EGR) as a result of the soot recirculation penalties [47]. It follows that for the tested fuels moderate levels of EGR are more favourable than higher rates.

3.7 Particle Size Distribution

Particle size distributions in number and mass concentration, total particle number and mean diameter size are shown in Figure 7 (a), (b), (c) and (d), respectively. The particle mass distribution was obtained from the particle number distribution using a size-dependant agglomerate density function as described by

Lapuerta et al [48]. The particle number concentration for B5 is the highest for all studied conditions. In fact the order of particle number emissions from highest to lowest exactly mirrors the order obtained for the soot emissions (see Figure 3 and 4). The decreased particle numbers for the oxygenated blends are often associated with the increased oxygen content that promotes particle precursors and particle oxidation [14][22],[31],[49]-[50] while the individual differences in particle numbers between the four blends can be explained by the same reasons as for the differences in soot emissions outlined above. As can be observed in Figure 7 (d), EGR greatly increases the number of particles and especially the proportion of larger particles as a result of lower oxygen availability and higher particle agglomeration. This increase is more noticeable in the case of B5 combustion compared to the oxygenated blends combustion. The oxygen contained in the fuel is more effective in fuel-air rich conditions (as those corresponding to high EGR rates) limiting particle formation as well as the particle recirculation penalty associated to high EGR rates [51].

Figure 7 (c) indicates that the mean particle diameter is smaller for the oxygenated blends. This has often been considered as one of the key drawbacks of oxygenated fuels. Smaller particles are more difficult to trap, they can penetrate the respiratory and even circulatory system, they remain airborne in the atmosphere for much longer than larger particles and they are more reactive due to their higher surface-to-volume ratio [14]. However, Figure 7 (a) indicates that the main reason for a reduction in mean particle diameter is a reduction in larger particle concentration [14],[22] which is also confirmed in the particle mass distributions. Therefore lower mean particle sizes for oxygenated blends are not actually a drawback but merely represent a reduction in larger particle emissions. This is a result of the lower particle formation and a corresponding lower likelihood of particle collision and the formation of larger particulate matter agglomerates.

3.8 Soot Oxidation Analysis

Soot oxidation is relevant in modern diesel after-treatment technology which involves the installation of diesel particulate filters (DPF). DPFs require active regeneration to maintain their function which incurs

significant fuel penalties. During these cleaning cycles the filter is heated and the accumulated soot is oxidised and dissipated as CO_2. In this research the oxidation temperature as well as the required activation energy of the produced soot particles is estimated using a TGA. The collected particulate matter samples were first devolatised by vaporising the adsorbed volatile organic material to isolate the soot effects. After cooling down the sample, the temperature is increased in an oxidant atmosphere to study the soot oxidation process. From the weight loss curve the temperature at which the maximum rate of soot oxidation occurs as well as the required soot activation energy can be calculated. For this purpose the method outlined by Rodríguez-Fernández et al. [42] was used which involves determining the activation energy from the following equation:

$$\ln\left(\frac{dm}{m\,dt}\right) = \ln\left(A\,p_{O_2}\right) - \frac{Ea}{RT} \qquad \text{Eq. (1)}$$

where m is the mass of soot, t the time, A is the pre-exponetial factor, p_{O_2} is the partial pressure of oxygen, R is the gas constant, T the temperature and Ea the activation energy.

Figure 8 (a) shows that the peak weight loss for B5-derived soot occurs at slightly higher temperatures than for soot produced by any of the oxygenated blends. This observation is confirmed in Figure 8 (b) which depicts the temperature for maximum rate of soot oxidation (second derivative of weight loss equal to zero). Additionally it can be seen that considerably less soot was produced in the combustion of 20DGE and 5DGE15E which qualitatively confirms the results obtained in the previous sections. Furthermore, the activation energy to oxidise the soot is also lower in the case of the oxygenated fuel blends. One of the reasons for this lower activation energy and soot oxidation temperature experienced for the oxygenated fuel blends may be the smaller amount of large soot particles which are less reactive and thus more difficult to oxidise. In addition, the potential presence of surface oxygen in the soot particles produced under the combustion of oxygenated fuels has also been reported to ease soot oxidation. Further details on this explanation can be found in a study by Song et al [52]. The lower soot and particulate matter emission level, the lower temperature for soot oxidation and the lower soot activation energy for oxidation obtained with the oxygenated blends will result in less frequent and more efficient DPF regeneration reducing the associated fuel penalty.

4. Conclusions

In this study the applicability of DGE as an oxygenated additive and a miscibility- and cetane-enhancer in ethanol-diesel blends was investigated. It was found that blends with up to 20% DGE content could be created that conform with existing diesel fuel standards as long as 5% RME was added to the base fuel ULSD (B5) as a means of improving the lubricity of the blend.

Adding DGE to diesel fuel resulted in improvements in all measured emissions compared to the B5 reference fuel. It should be emphasised that both soot and NO_x reductions were obtained simultaneously. While the fuel-born oxygen reduced soot emission, improvements in NO_x were obtained as a result of a lower premixed combustion. It can be also established that DGE improves some of the major shortcomings of e-diesel. Small additions of DGE greatly enhance blend stability and improve the auto ignition properties of the resulting blend due to its high cetane number. All blends produced reductions in PM number concentrations and displayed improved soot oxidation behaviour which provides benefits for DPF regeneration.

It can be concluded that in this research various partly renewable diesel blends can provide considerable environmental and energy efficiency improvements while offering flexible combustion patterns. 20DGE displayed the best overall emission characteristics with reductions in all investigated emissions while 5DGE15E followed with a similarly favourable soot/ NO_x trade-off. However differences in fuel properties (e.g. lubricity), combustion patterns, price and the share of renewable blend components exist between the two blends. Ultimately, the choice of which blend to use lies with the end-user and depends on the specific combustion requirements.

Acknowledgements

With thanks to Advantage West Midlands and the European Regional Development Fund, funders of the Science City Research Alliance Energy Efficiency project, a collaboration between the Universities of Birmingham and Warwick. Moreover Shell Global Solutions is thanked for providing the ULSD and ethanol fuels.

References

[1] Luque R. Algal biofuels: the eternal promise?. *Energy Environ. Sci.* 2010;3:254-7.

[2] Stucki S, Vogel F, Ludwig C, Hiduc AG, Brandenberger M. Catalytic gasification of algae in supercritical water for biofuel production and carbon capture. *Energy Environ. Sci.* 2009;2:535-41.

[3] Dupont, J, Suarez, PAZ, Meneghetti, MR, Simoni, MP, Meneghetti, MP. Catalytic production of biodiesel and diesel-like hydrocarbons from triglycerides. *Energy Environ. Sci.* 2009;2:1258-65.

[4] David K, Ragauskas AJ. Switchgrass as an energy crop for biofuel production: A review of its ligno-cellulosic chemical properties. *Energy Environ. Sci.* 2010;3:1182-90.

[5] Herreros JM, Jones A, Sukjit E, Tsolakis A. Blending lignin-derived oxygenate in enhanced multi-component diesel fuel for improved emissions. *Appl. Energ.* 2014;116:58–65.

[6] Yasin MHM, Yusaf T, Mamat TR, Yusop AF. Characterization of a diesel engine operating with a small proportion of methanol as a fuel additive in biodiesel blend. *Appl. Energ.* 2014;114:865-73.

[7] Park SH, Yoon SH, Lee CS. HC and CO emissions reduction by early injection strategy in a bioethanol blended diesel-fueled engine with a narrow angle injection system. *Appl. Energ*. 2013;107:81-8.

[8] Zhang Z-H, Balasubramanian R. Influence of butanol addition to diesel-biodiesel blend on engine performance and particulate emissions of a stationary diesel engine. *Appl. Energ*. 2014;119:530-6.

[9] Campos-Fernández J, Arnal JM, Gómez J, Dorado MP. A comparison of performance of higher alcohols/diesel fuel blends in a diesel engine. *Appl. Energ*. 2012;95:267-75.

[10] Hulwan DB, Joshi SV. Performance, emission and combustion characteristics of a multicylinder DI diesel engine running on diesel-ethanol-biodiesel blends of high ethanol content. *Appl. Energ.* 2011;88:5042-55.

[11] McCormick RL, Ross JD, Graboski MS. Effect of Several Oxygenates on Regulated Emissions from Heavy-Duty Diesel Engines. *Environ. Sci. Technol.* 1997;31:1144−50.

[12] Hansen AC, Zhang Q, Lyne PLW. Ethanol-diesel fuel blends – a review. *Bioresource Technol*. 2006;96:277-85.

[13] Waterland LR, Venkatesh S, Unnasch S. Safety and performance assessment of ethanol/diesel blends (e-diesel). National Renewable Energy Laboratory 2003. Colorado. USA.

[14] Lapuerta M, Armas O, Herreros JM. Emissions from a diesel-bioethanol blend in an automotive diesel engine. *Fuel*. 2008;87:25-31.

[15] Lapuerta M, Armas O, Garcia-Contreras R. Stability of diesel-ethanol blends for the use in diesel engines. *Fuel*. 2007;86:1351-57.

[16] Xing-Cai L, Jiang-Guang Y, Wu-gao Z, Zhen H. Effect of cetane number improver on heat release rate and emissions of high speed diesel engine fuelled with ethanol-diesel blend fuel. *Fuel*. 2004;83:2013-20.

[17] Beatrice C, Napolitano P, Guido C. Injection parameter optimization by DoE of a light-duty diesel engine fed by Bio-ethanol/RME/diesel blend. *Appl. Energ*. 2014;113:373-84.

[18] Guido C, Beatrice C, Napolitano P. Application of bioethanol/RME/diesel blend in a Euro5 automotive diesel engine: Potentiality of closed loop combustion control technology. *Appl. Energ*. 2013;102:13-23.

[19] Miyamoto N, Ogawa H, Nurun NM, Obata K, Arima T. Smokeless, Low NOx, High Thermal Efficiency, and Low Noise Diesel Combustion with Oxygenated Agents as Main Fuel. *SAE Paper*. 1998;980605.

[20] Ren Y, Huang Z, Miao H, Jiang D, Zeng K, Liu B, Wang X. Effect of the addition of diglyme in diesel fuel on combustion and emission in a compression-ignition engine. *Energy and Fuels*. 2007;21(5):2573-83.

[21] Di Y, Chueng CS, Huang Z. Experimental investigation of particulate emissions from a diesel engine fueled with ultralow-sulfur diesel fuel blended with diglyme. *Atmospheric Environment*. 2010;44(1):55-63.

[22] Gill SS, Tsolakis A, Herreros JM, York APE. Diesel emission improvements through the use of biodiesel or oxygenated blending components. *Fuel*. 2012;95:578-86.

[23] Cheng AS, Upatnieks A, Mueller CJ. Investigation of Fuel Effects on Dilute, Mixing-Controlled Combustion in an Optical Direct-Injection Diesel Engine. *Energ. Fuel*. 2007;21:1989-2002.

[24] Upatnieks A, Mueller CJ. Clean Controlled DI Diesel Combustion Using Dilute, Cool Charge Gas and a Short-Ignition Delay, Oxygenated Fuel. *SAE Paper*. 2005;2005-01-0363.

[25] Upatnieks A, Mueller CJ, Martin GC. The Influence of Charge Gas Dilution and Temperature on DI Diesel Combustion Processes Using a Short-Ignition Delay, Oxygenated Fuel. *SAE Paper*. 2005;2005-01-2088.

[26] Rakopoulos DC, Rakopoulos CD, Giakoumis EG, Dimaratos AM. Characteristics of performance and emissions in high-speed direct injection diesel engine fueled with diethyl ether/diesel fuel blends. *Energy*. 2012;43:214-24.

[27] EN 590:2009 Automotive Fuels – Diesel – Requirements and test methods.

[28] EN ISO 12156-1:2006 Diesel fuel — Assessment of lubricity using the high-frequency reciprocating rig (HFRR).

[29] Lapuerta M, Garcia-Contreras R, Agudelo JR. Lubricity of Ethanol-Biodiesel-Diesel Fuel Blends. *Energ. Fuel*. 2010;24:1374-9.

[30] Sukjit E, Herreros JM, Piaszyk J, Dearn KD, Tsolakis A. Finding Synergies in Fuels Properties for the Design of Renewable Fuels − Hydroxylated Biodiesel Effects on Butanol-Diesel Blends. *Environ. Sci. Technol*. 2013;47:3535−42.

[31] Sukjit E, Herreros JM, Dearn KD, Garcia-Contreras R, Tsolakis A. The effect of the addition of individual methyl esters on the combustion and emissions of ethanol. *Energy*. 2012;42:364-74.

[32] Li XX, Liu YX, Wei XH. Density, Viscosity, and Surface Tension at 293.15 K and Liquid-Liquid Equilibria from 301.15 K to 363.15 K under Atmospheric Pressure for the Binary Mixture of Diethylene Glycol Diethyl Ether + Water. *J Chem. Eng. Data*. 2004;49:1043-5.

[33] Lapuerta M, Garcia-Contreras R, Campos-Fernández J, Pilar Dorado MP. Stability, Lubricty, Viscosity and Cold-Flow Properties of Alcohol-Diesel Blends. *Energ. Fuel*. 2010;24:4497-502.

[34] Lapuerta M, Armas O, Rodríguez-Fernández J. Effect of biodiesel fuels on diesel engine emissions- *Prog. Energ. Combust.* 2008;34:198-223.

[35] Ren Y, Huang Z, Miao H, Jiang D, Zeng K, Liu B, Wang X. Combustion and emissions characteristics of a Direct-Injection diesel engine fueled with diesel-diethyl adipate blends. *Energ. Fuel*. 2007;21:1474-82.

[36] Lapuerta M, Rodríguez-Fernández J, Font de Mora E. Correlation for the estimation of the cetane number of biodiesel fuels and implications on the iodine number. *Energ. Policy*. 2009;37:4337–44.

[37] Knothe G. Dependence of biodiesel fuel properties on the structure of fatty acid alkyl esters. *Fuel. Process. Technol.* 2005;86:1059–70.

[38] Rounce P, Tsolakis A, Rodríguez-Fernández J, York APE, Cracknell RF, Clark RH. Diesel Engine Performance and Emissions when First Generation Meets Next Generation Biodiesel. *SAE Paper*. 2009;2009-01-1935.

[39] Hsu BD. Practical Diesel-Engine Combustion Analysis. Warrendale, PA (USA): Society of Automotive Engineers (SAE) Inc.; 2002.

[40] Rakopoulos CD, Hountalas DT, Zannis TC, Levendis YA. Operational and Environmental evaluation of diesel engines burning oxygen-enriched intake air or oxygen-enriched fuels: a review. *SAE Paper*. 2004;2004-01-2924.

[41] Monyem A, Van Gerpen JH, Canakci M. The effect of timing and oxidation on emissions from biodiesel-fuelled engines, *Trans ASAE*. 2001;44:35-42.

[42] Ullman TL, Spreen KB, Mason RL. Effects of cetane number, cetane improver, aromatics and oxygenates on 1994 heavy-duty diesel engine emissions. *SAE Paper*. 1994;941020.

[43] Shi X, Yu Y, He H, Shuai S, Wang J, Li R. Emission characteristics using methyl soyate-ethanol-diesel fuel blends on a diesel engine. *Fuel*. 2005;84:1543-9.

[44] Hoekman SK, Robbins C. Review of the effects of biodiesel on NOx emissions. *Fuel. Process. Technol.* 2012;96:237-49.

[45] Rodríguez-Fernandez J, Oliva F, Vazquez RA. Characterization of the Diesel Soot Oxidation Process through an Optimized Thermogravimetric Method. *Energ. Fuel*. 2011;25:2039–48.

[46] Westbrook CK, Pitz WJ, Curran HJ. Chemical kinetic modelling study of the effect of oxygenated hydrocarbons on soot emissions from diesel engines. *J. Phys. Chem. A.* 2006;21:6912-22.

[47] Gill SS, Turner D, Tsolakis A, York APE. Controlling soot formation with filtered EGR for diesel and biodiesel fuelled engines. *Environ. Sci. Technol*. 2012;46(7):4215−22.

[48] Lapuerta M, Armas O, Gómez A. Diesel particle size distribution estimation from digital image analysis. *Aerosol Sci Tech*. 2003;37:369-81.

[49] Pinzi S, Rounce P, Herreros JM, Tsolakis A, Dorado MP. The effect of biodiesel fatty acid composition on combustion and diesel engine exhaust emissions. *Fuel*. 2013;104:170-82.

[50] Nord KE, Haupt D. Reducing the Emission of Particles from a Diesel Engine by Adding an Oxygenate to the Fuel. *Environ. Sci. Technol*. 2005;39:6260-5.

[51] Gill SS, Herreros JM, Tsolakis A, Turner DM, Miller E, York APE. Filtered EGR-a step towards an improved NO_X/soot trade-off for DPF regeneration. RSC Adv. 2012;2(27):10400-8.

[52] Song J, Alam M, Boehman AL, Kim U. Examination of the oxidation behavior of biodiesel soot. *Combust. Flame*. 2006;146(4):589−604.

Table

Table 1: Fuel properties

	Test Method	B5	DGE	Ethanol	20DGE	15DGE5E	10DGE10E	5DGE15E
Chemical Formula		$C_{14.18}H_{26.42}O_{0.07}$	$C_8H_{18}O_3$	C_2H_6O	$C_{12.63}H_{24.31}O_{0.81}$	$C_{11.08}H_{21.56}O_{0.72}$	$C_{9.85}H_{19.37}O_{0.65}$	$C_{8.85}H_{17.58}O_{0.59}$
Molar mass [g/mol]		197.76	162	46	186.12	163.69	145.85	131.34
Cetane Number[a]		53.94	140**Error! Reference source not found.**	8[29]	71.18	68.89	62.29	55.69
Cetane Number[b]		53.93	140**Error! Reference source not found.**	8[29]	75.49	60.46	48.52	38.80
Viscosity at 40 °C [cSt]	ISO 3105	2.57	1.18	1.13[31]	2.27	2.28	2.29	2.29
Density at 15 °C [kg/m³][c]	ISO 12185	829.87	908[32]	789[31]	845.70	827.70	833.70	839.70
LHV [MJ/kg][a]	ISO 1928	42.99	31.40	26.83[33]	40.50	40.35	40.19	40.04
Lubricity at 60 °C [µm]	ISO 12156-1	294	747	656	431	414	411	403
C [wt%]		86.02	59.26	52.17	80.57	80.39	80.20	80.02
H [wt%]		13.40	11.11	13.04	12.97	13.07	13.18	13.29

O [wt%]	0.58	29.63	34.78	6.46	6.54	6.62	6.70

[a] estimated based on mass fraction
[b] estimated based on molar fraction
[c] estimated based on volumetric fraction

Figure Captions

Figure 1: Corrected wear scar of DGE-ULSD blends, DGE-B5 blends and the test-blends

Figure 2: (a) Indicated engine thermal efficiency, (b) cylinder pressure and ROHR for 5 bar IMEP and 0%EGR

Figure 3: Emissions at 3 bar IMEP (a) 0% EGR, (b) 20% EGR

Figure 4: Emissions at 5 bar IMEP and (a) 0% EGR, (b) 20% EGR

Figure 5: Soluble Organic Fraction (SOF) for all operating conditions

Figure 6: NO_x/Soot trade-off under EGR conditions (5 bar IMEP)

Figure 7: Fuel effects on (a) particle size distribution, (b) mass distribution, (c) total particle number and mean diameter at 0% EGR and 5 bar IMEP, (d) total particle mass with varying EGR

Figure 8: (a) Derivative dry soot weight loss, (b) oxidation temperature and soot activation energy (Ea) at 5bar IMEP and 0% EGR

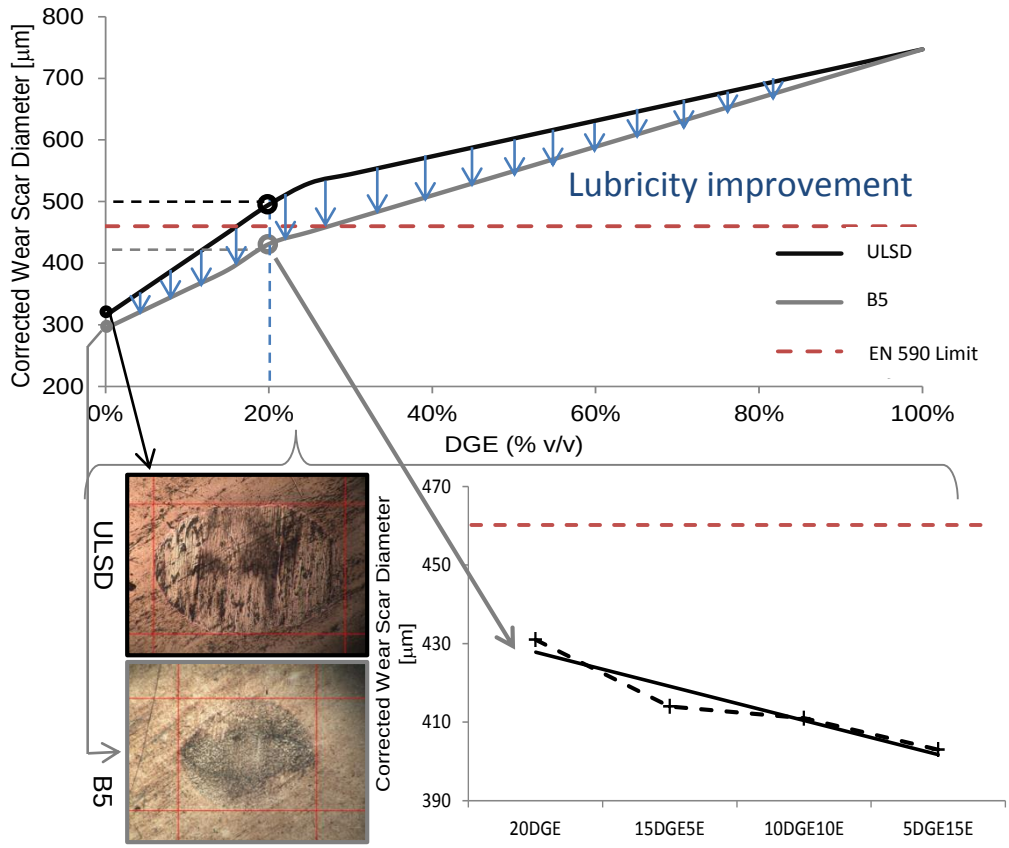
Corrected Wear Scar Diameter [µm]
800
700
600
500
400
300
200
Lubricity improvement
ULSD
B5
EN 590 Limit
0%
20%
40%
60%
80%
100%
DGE (% v/v)
ULSD
B5
Corrected Wear Scar Diameter [µm]
470
450
430
410
390
20DGE
15DGE5E
10DGE10E
5DGE15E

Figure 1

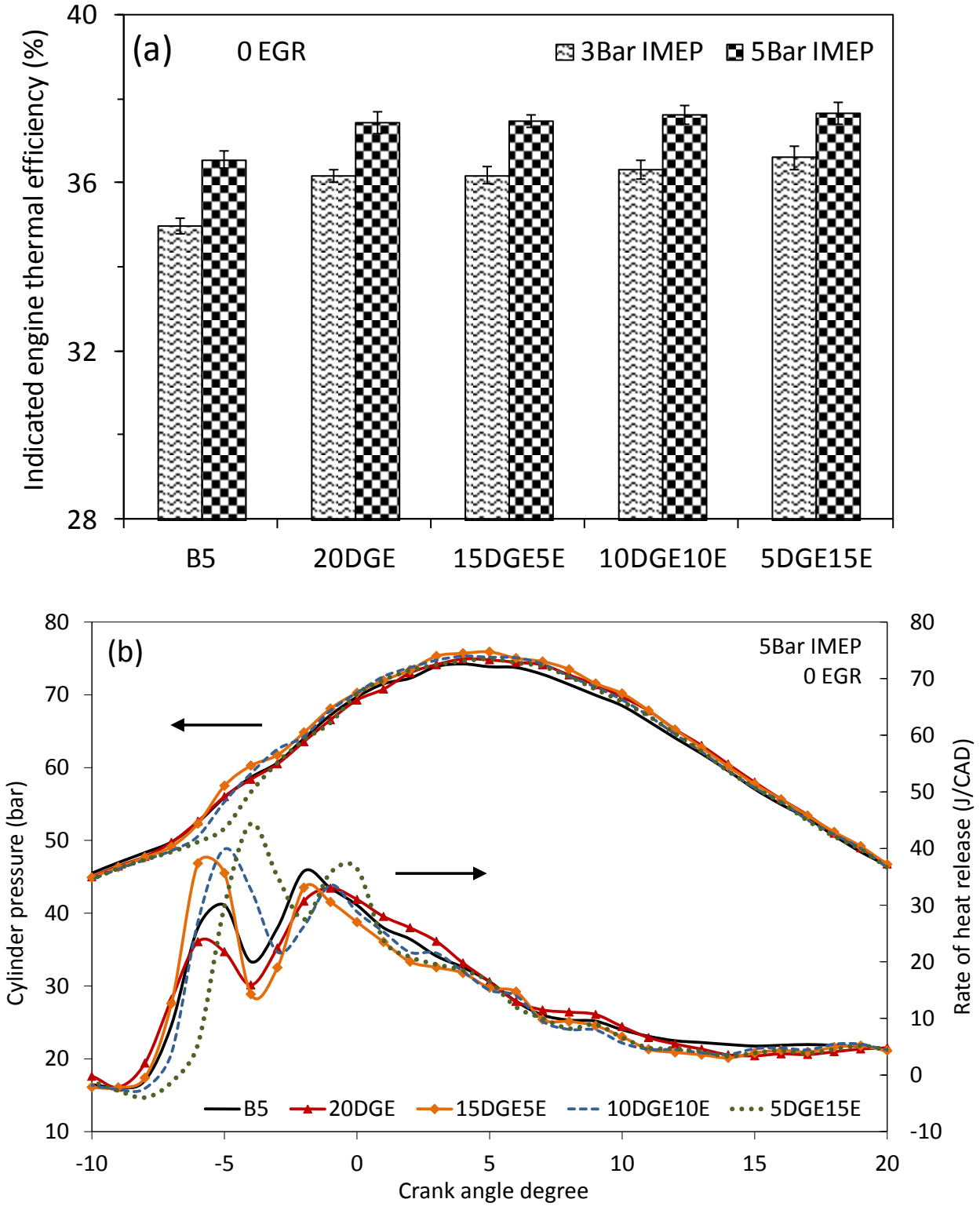
(a)
0 EGR
3Bar IMEP
5Bar IMEP
Indicated engine thermal efficiency (%)
40
36
32
28
B5
20DGE
15DGE5E
10DGE10E
5DGE15E
(b)
5Bar IMEP
0 EGR
Cylinder pressure (bar)
Rate of heat release (J/CAD)
Crank angle degree
B5
20DGE
15DGE5E
10DGE10E
5DGE15E

Figure 2

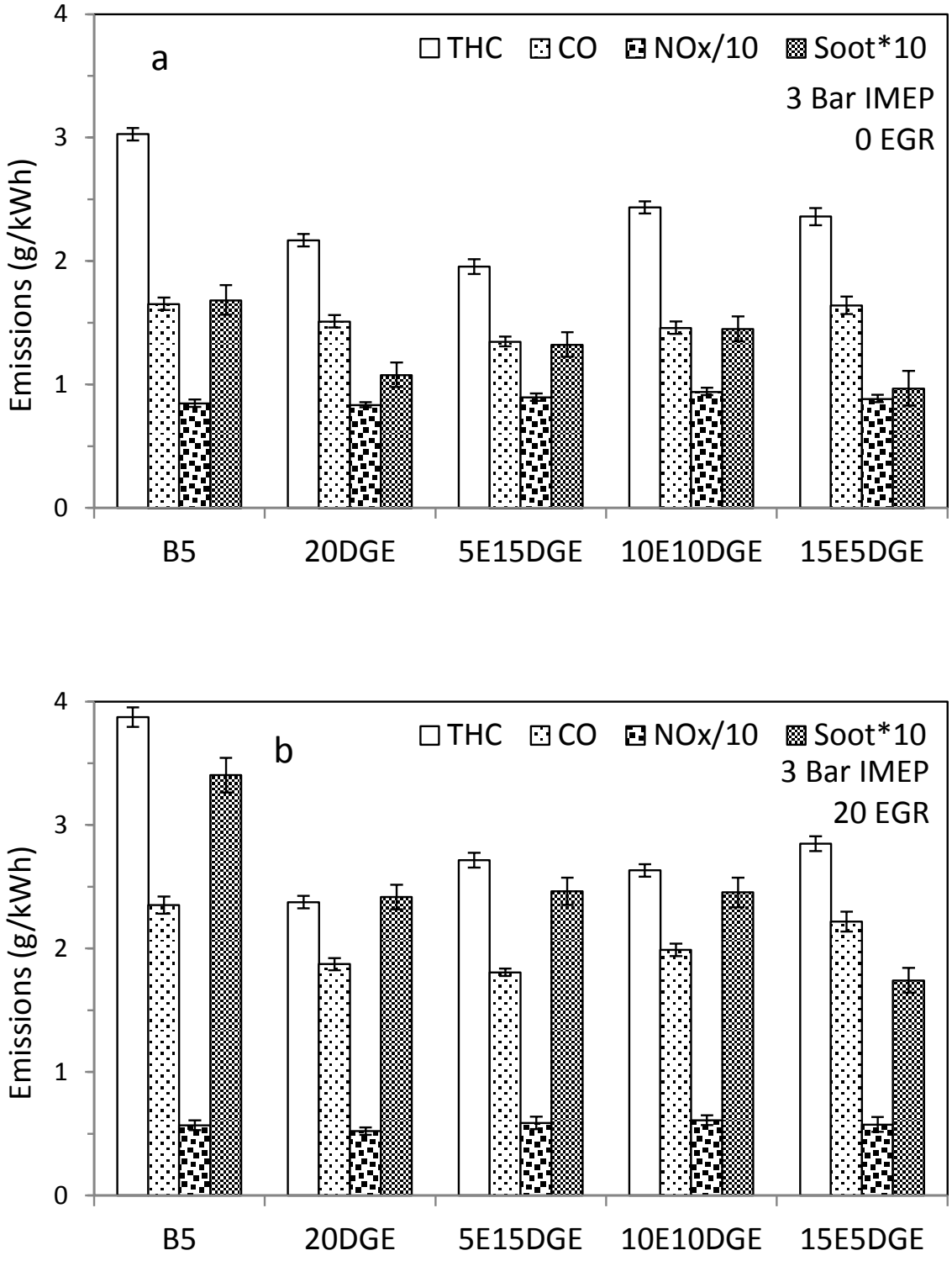
a
THC
CO
NOx/10
Soot*10
3 Bar IMEP
0 EGR
Emissions (g/kWh)
0
1
2
3
4
B5
20DGE
5E15DGE
10E10DGE
15E5DGE
b
THC
CO
NOx/10
Soot*10
3 Bar IMEP
20 EGR
Emissions (g/kWh)
0
1
2
3
4
B5
20DGE
5E15DGE
10E10DGE
15E5DGE

Figure 3

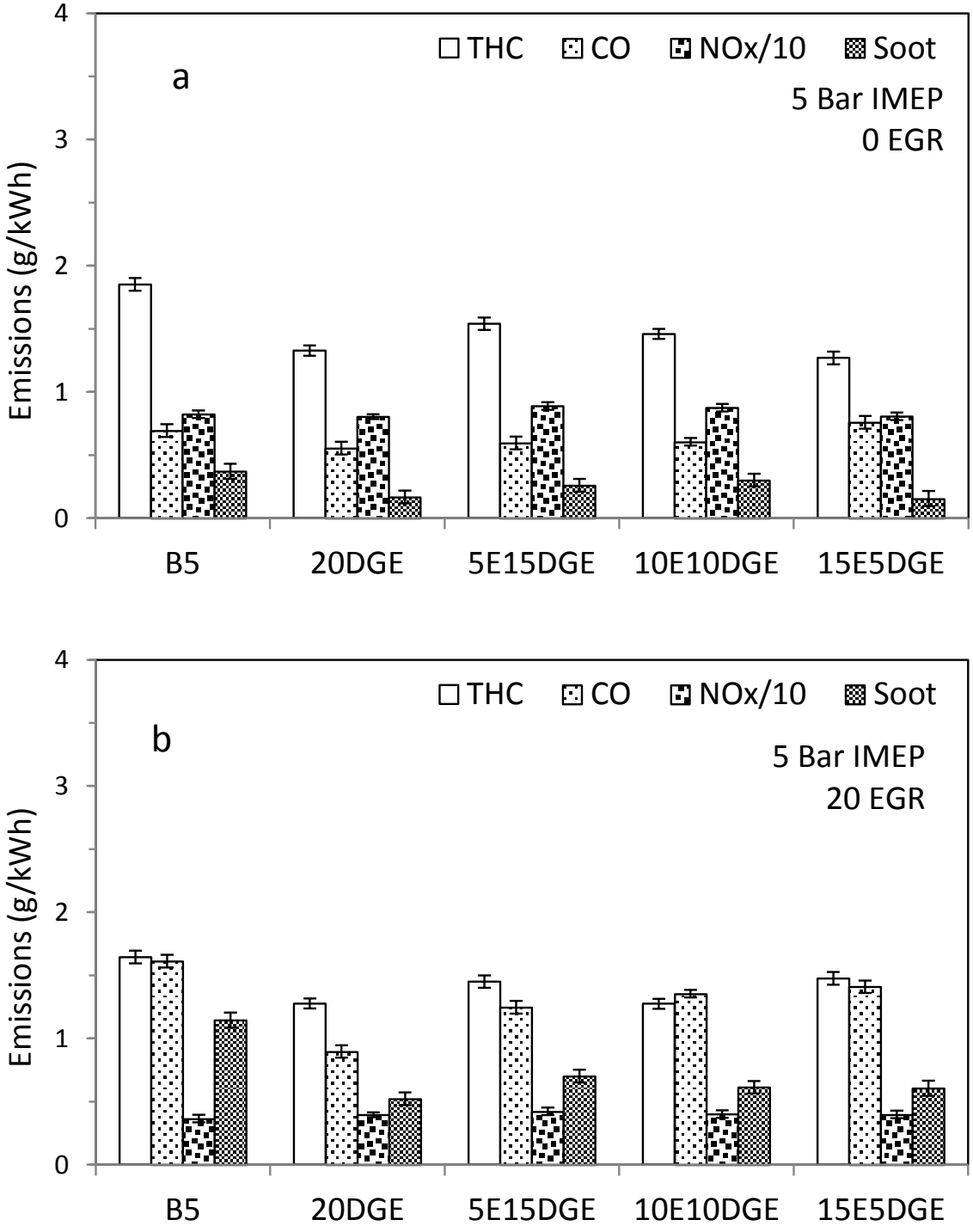
a
THC
CO
NOx/10
Soot
5 Bar IMEP
0 EGR
Emissions (g/kWh)
0
1
2
3
4
B5
20DGE
5E15DGE
10E10DGE
15E5DGE
b
THC
CO
NOx/10
Soot
5 Bar IMEP
20 EGR
Emissions (g/kWh)
0
1
2
3
4
B5
20DGE
5E15DGE
10E10DGE
15E5DGE

Figure 4

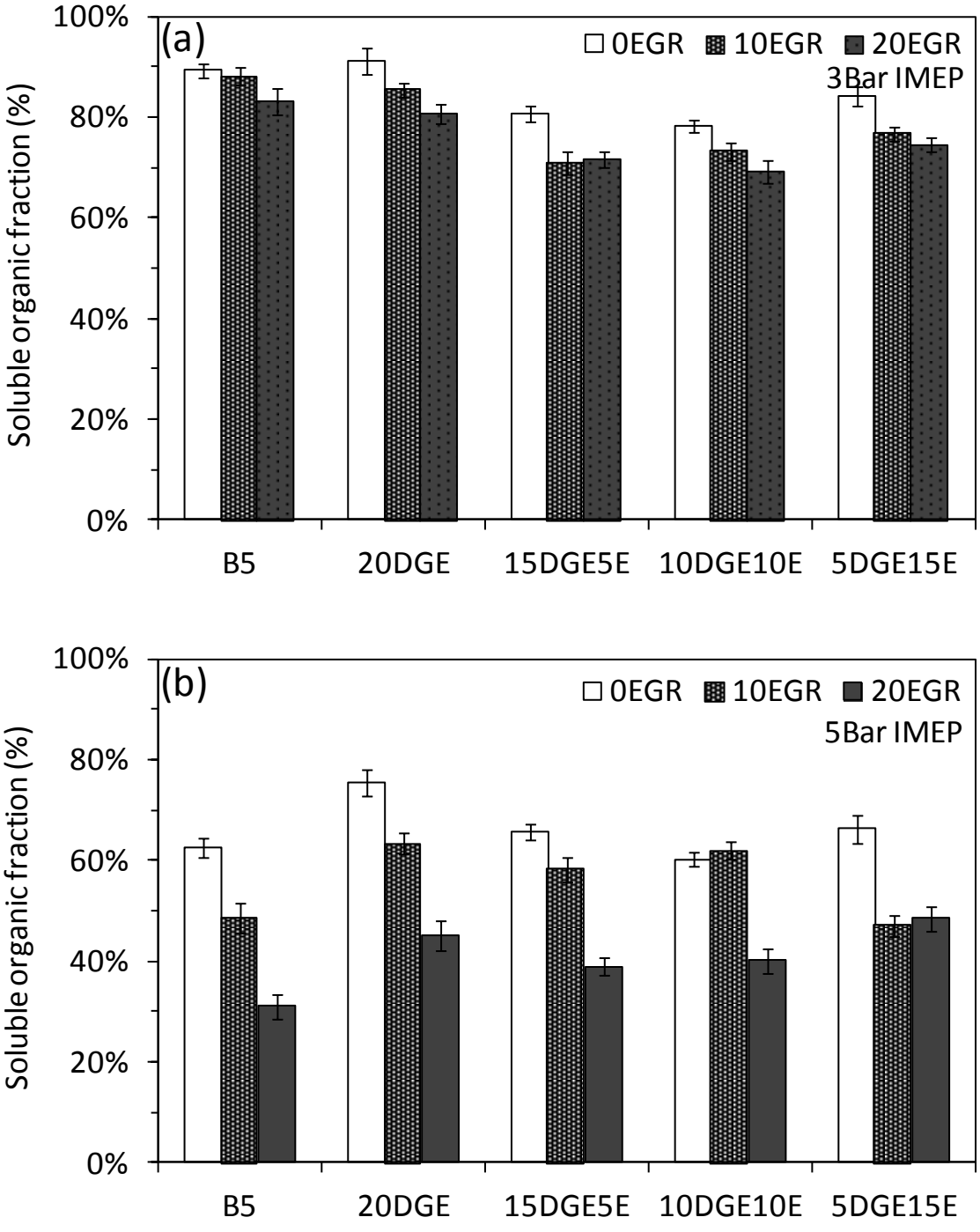
(a)
0EGR
10EGR
20EGR
3Bar IMEP
Soluble organic fraction (%)
100%
80%
60%
40%
20%
0%
B5
20DGE
15DGE5E
10DGE10E
5DGE15E
(b)
0EGR
10EGR
20EGR
5Bar IMEP
Soluble organic fraction (%)
100%
80%
60%
40%
20%
0%
B5
20DGE
15DGE5E
10DGE10E
5DGE15E

Figure 5

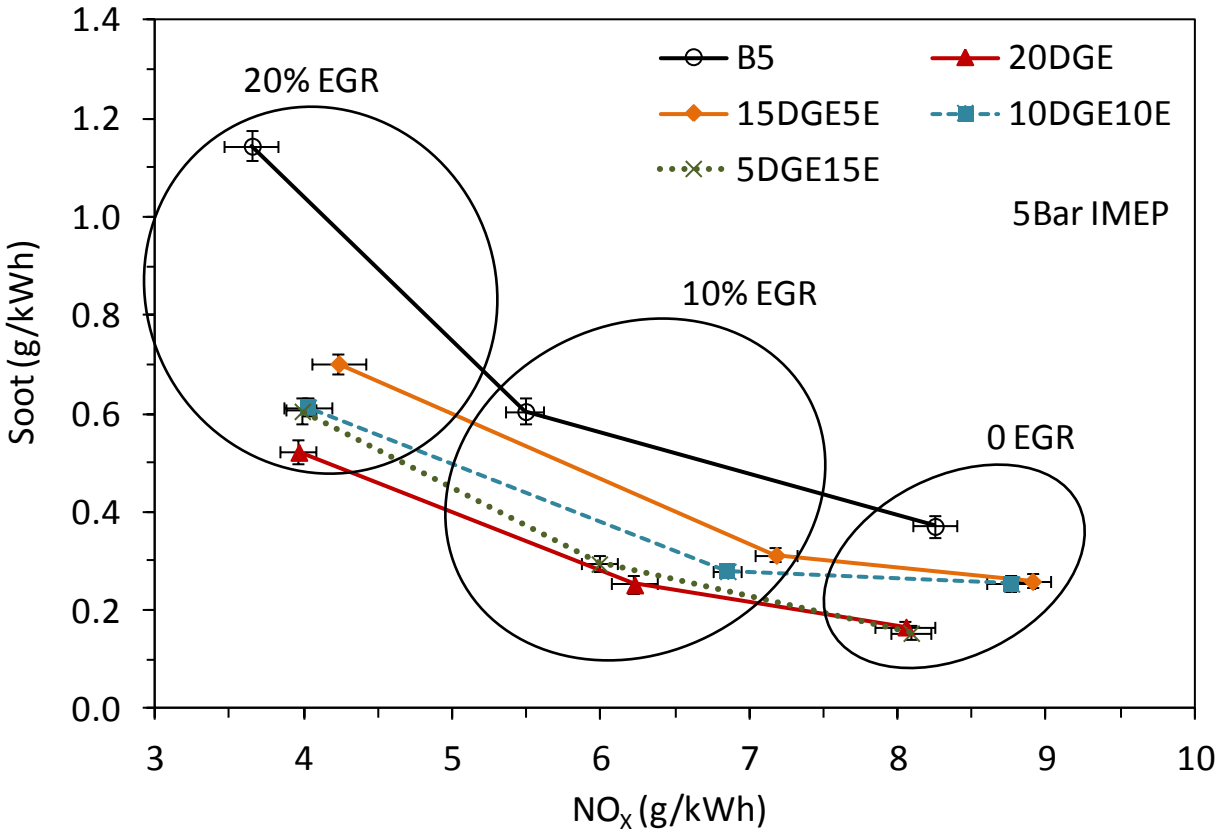
1.4
1.2
1.0
0.8
0.6
0.4
0.2
0.0
Soot (g/kWh)
3
4
5
6
7
8
9
10
NOx (g/kWh)
20% EGR
10% EGR
0 EGR
B5
20DGE
15DGE5E
10DGE10E
5DGE15E
5Bar IMEP

Figure 6

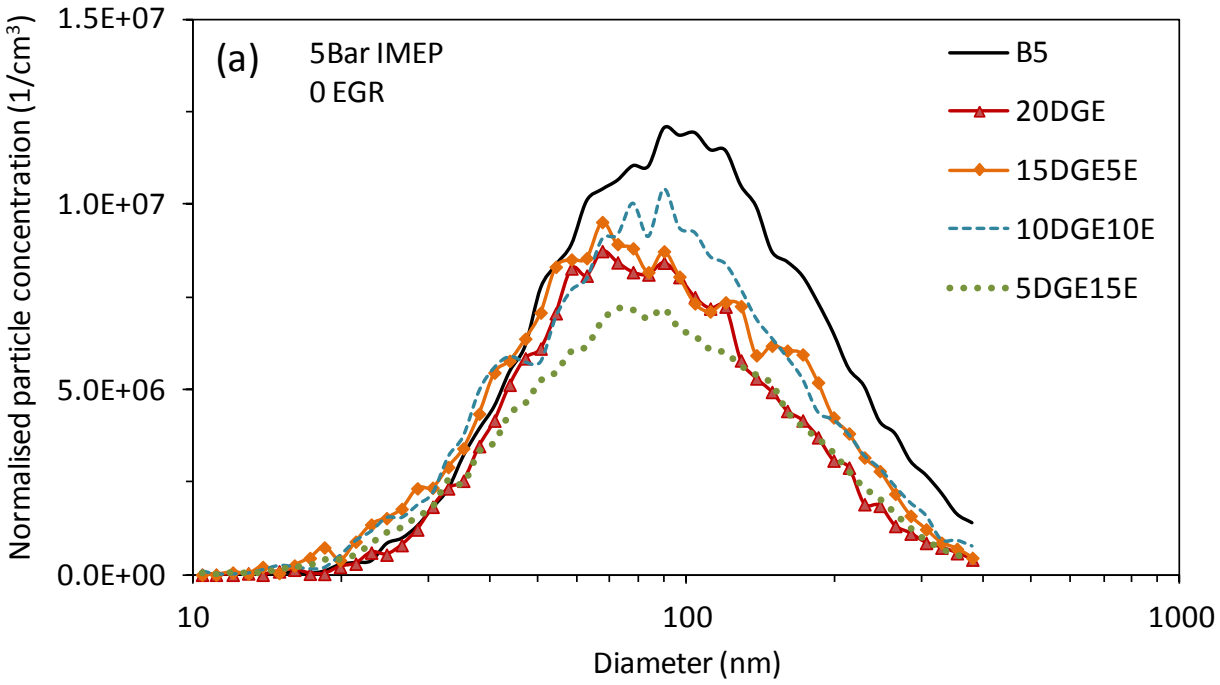
(a)
5Bar IMEP
0 EGR
B5
20DGE
15DGE5E
10DGE10E
5DGE15E
Normalised particle concentration (1/cm³)
1.5E+07
1.0E+07
5.0E+06
0.0E+00
10
100
1000
Diameter (nm)

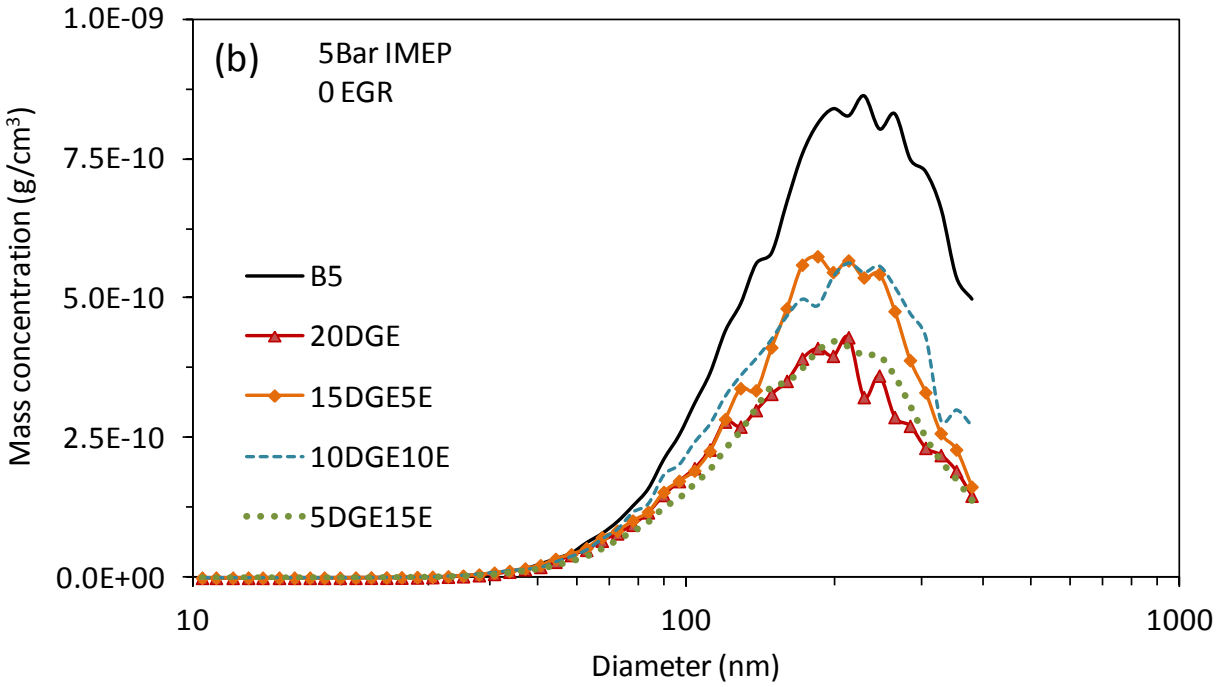
(b)
5Bar IMEP
0 EGR
B5
20DGE
15DGE5E
10DGE10E
5DGE15E
Mass concentration (g/cm³)
1.0E-09
7.5E-10
5.0E-10
2.5E-10
0.0E+00
10
100
1000
Diameter (nm)

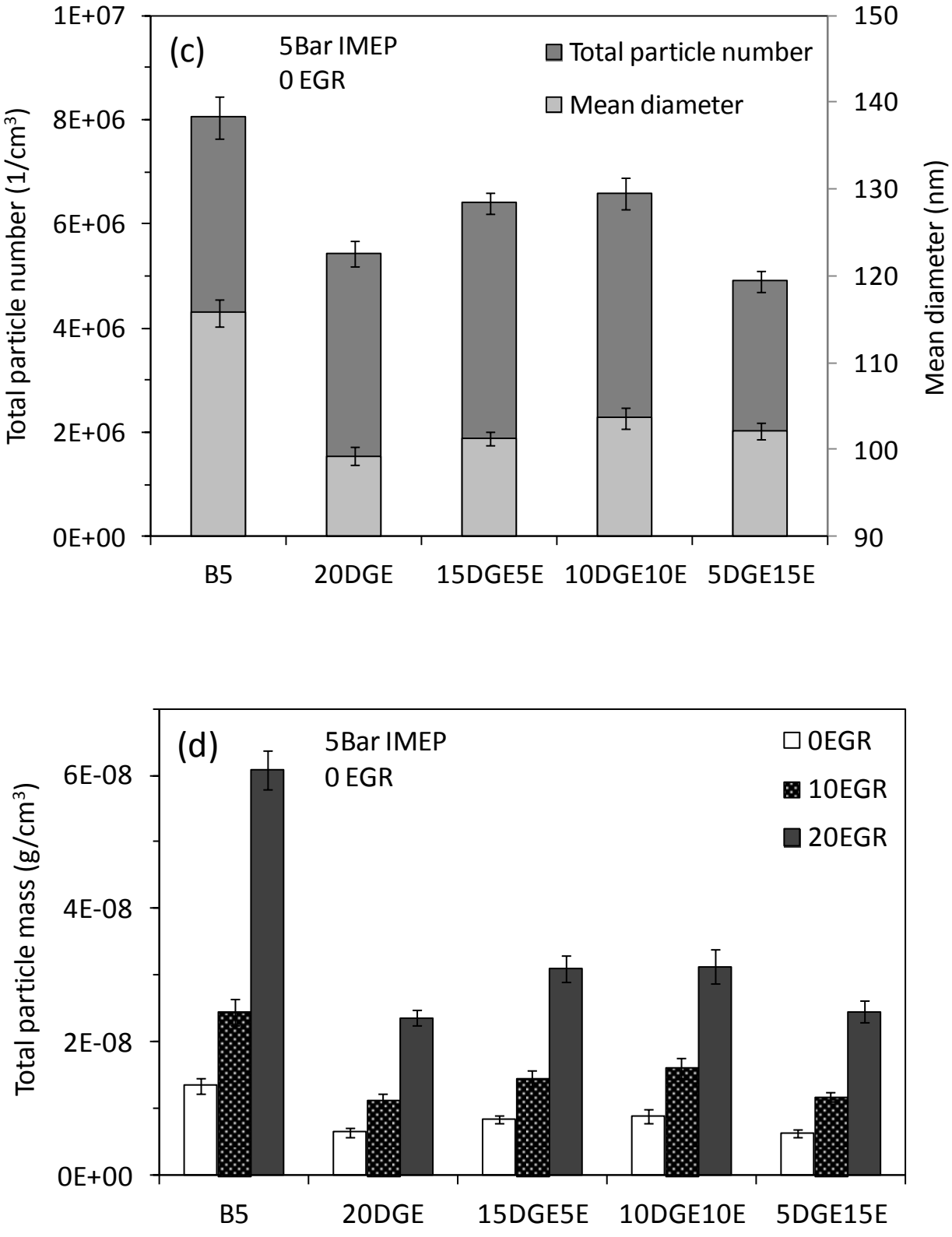
(c)
5Bar IMEP
0 EGR
Total particle number
Mean diameter
Total particle number (1/cm³)
Mean diameter (nm)
1E+07
8E+06
6E+06
4E+06
2E+06
0E+00
150
140
130
120
110
100
90
B5
20DGE
15DGE5E
10DGE10E
5DGE15E
(d)
5Bar IMEP
0 EGR
0EGR
10EGR
20EGR
Total particle mass (g/cm³)
6E-08
4E-08
2E-08
0E+00
B5
20DGE
15DGE5E
10DGE10E
5DGE15E

Figure 7

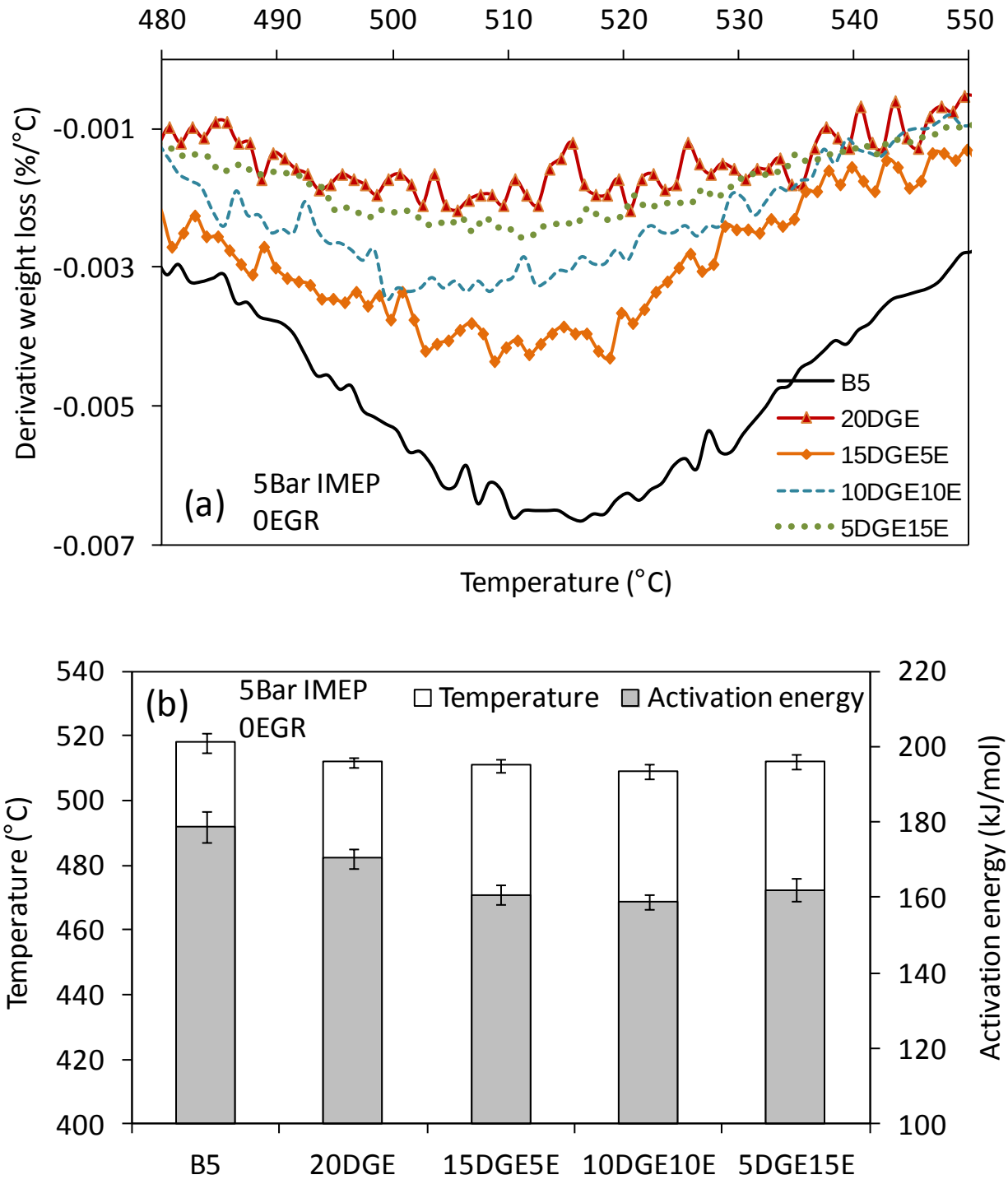
480
490
500
510
520
530
540
550
-0.001
-0.003
-0.005
-0.007
Derivative weight loss (%/°C)
Temperature (°C)
(a)
5Bar IMEP
0EGR
B5
20DGE
15DGE5E
10DGE10E
5DGE15E
(b)
5Bar IMEP
0EGR
Temperature
Activation energy
540
520
500
480
460
440
420
400
Temperature (°C)
220
200
180
160
140
120
100
Activation energy (kJ/mol)
B5
20DGE
15DGE5E
10DGE10E
5DGE15E

Figure 8